

## Supplementary Materials for

### **PCGF6 controls neuroectoderm specification of human pluripotent stem cells by activating SOX2 expression**

**This PDF file includes:**

Supplementary Figures 1 to 5

Supplementary Tables 1 to 2

## **Index of Supplemental Information**

### **Supplementary Figures**

Supplementary Figure 1. Deletion of PCGF6 does not affect pluripotency maintenance of human PSCs.

Supplementary Figure 2. PCGF6 regulates endoderm differentiation of human PSCs.

Supplementary Figure 3. PCGF6 knockout delays pluripotency exits during neuroectoderm differentiation.

Supplementary Figure 4. SRE-deficiency blocks neuroectoderm differentiation of human PSCs.

Supplementary Figure 5. Analyses of the co-occupancy of PCGF6 and MYC.

### **Supplementary Tables**

Supplementary Table 1. Primers for RT-qPCR analyses

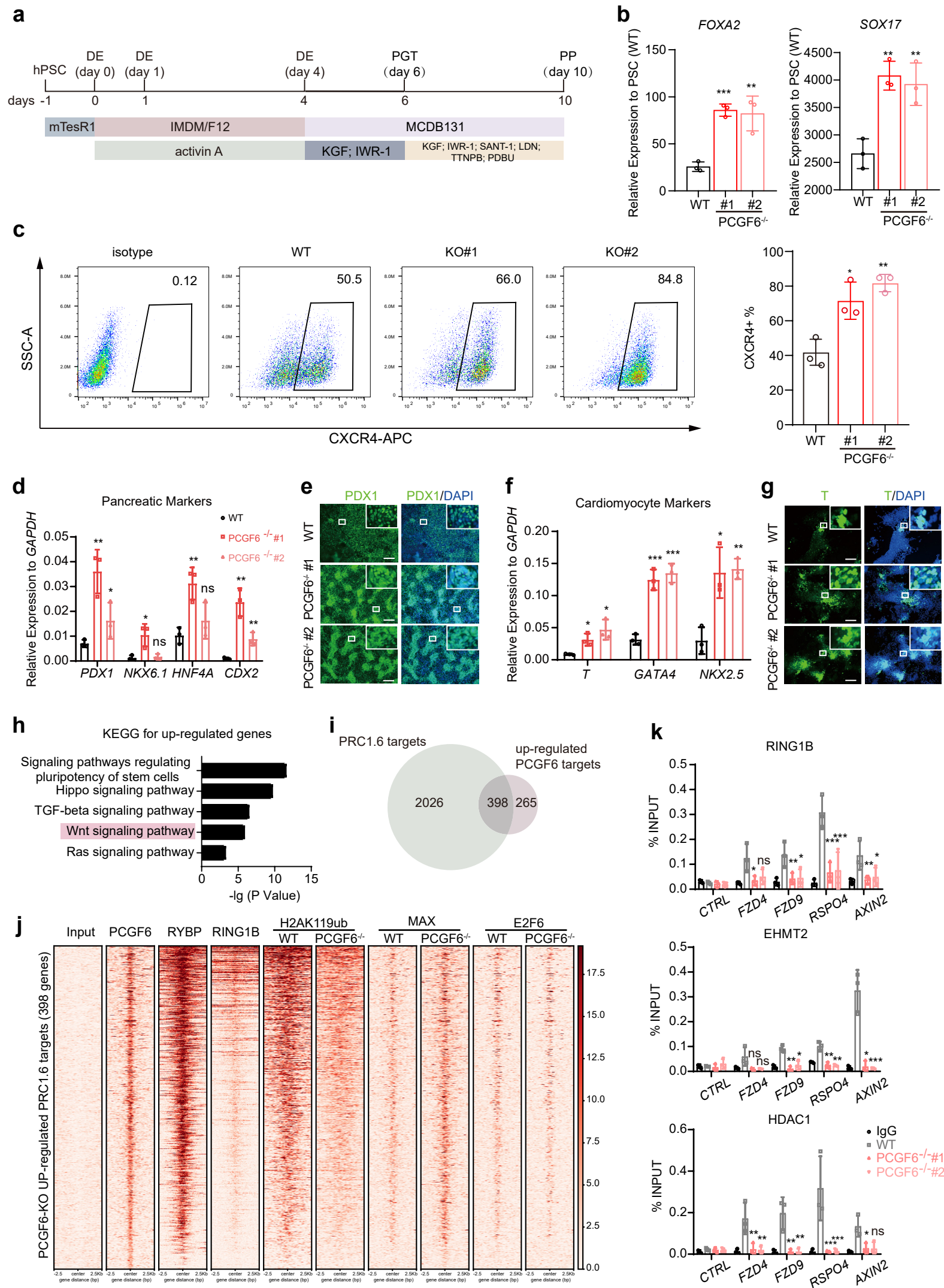
Supplementary Table 2. Primers for ChIP-qPCR analyses





**Supplementary Figure 1. Deletion of PCGF6 does not affect pluripotency maintenance of human PSCs.**

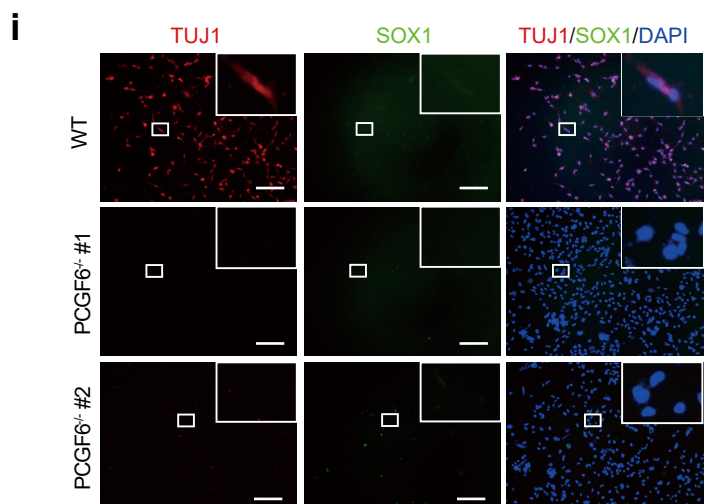
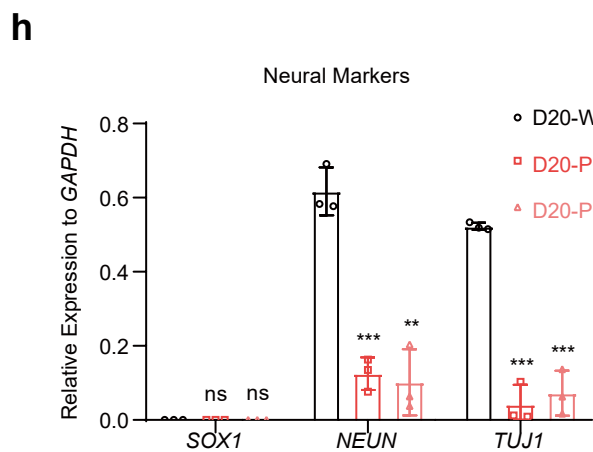
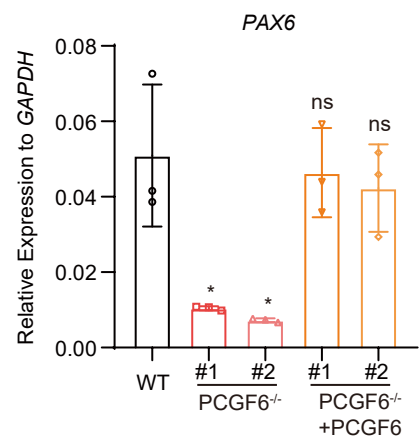
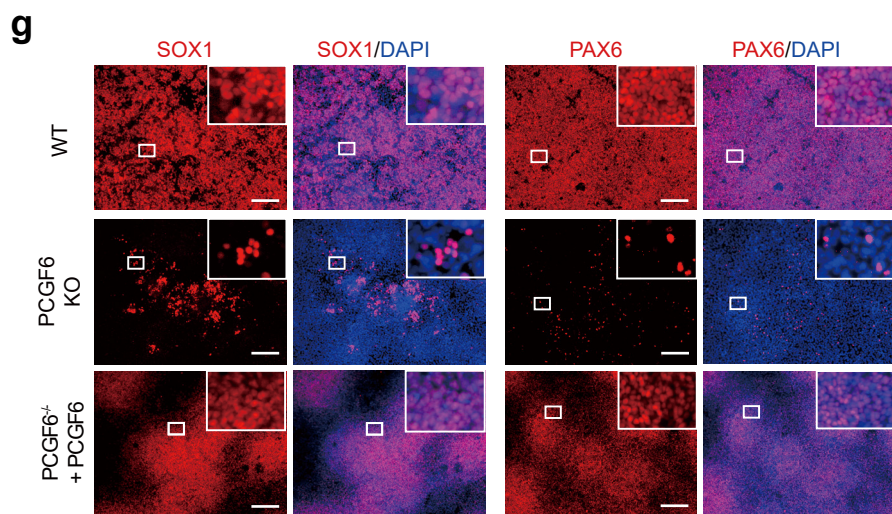
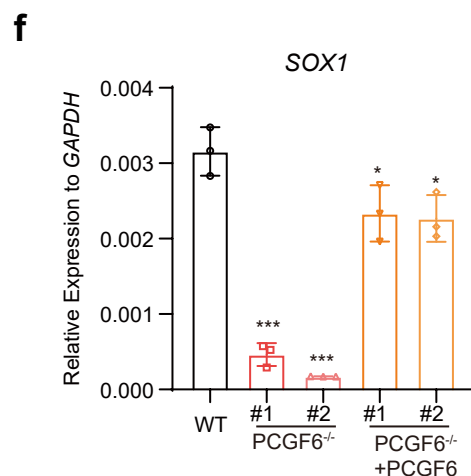
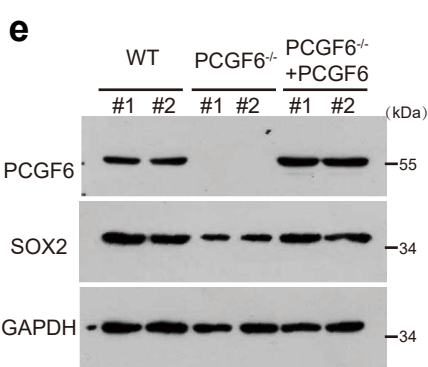
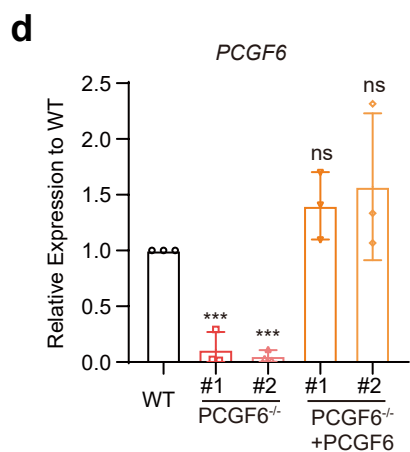
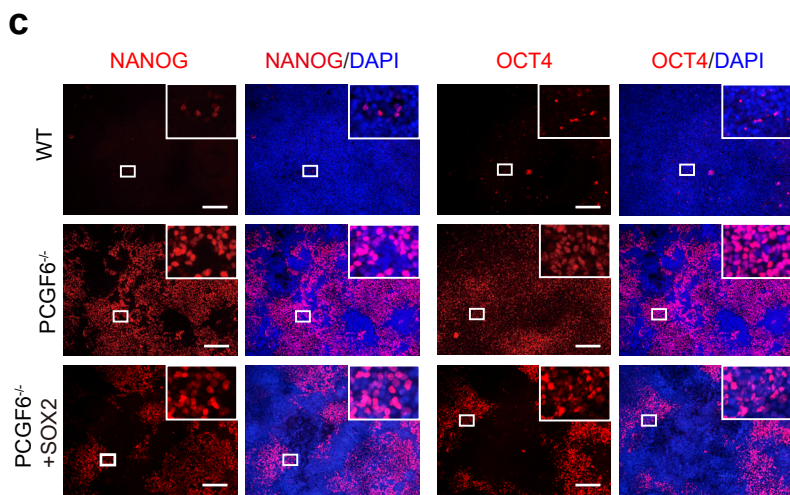
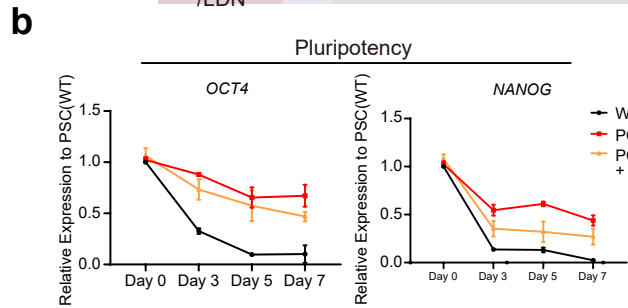
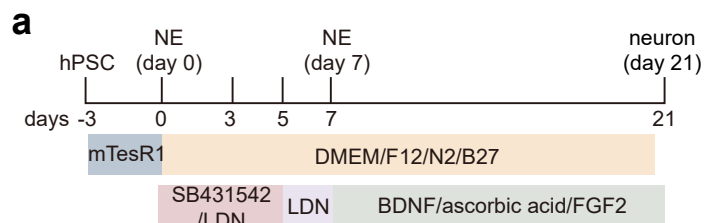
**a.** Schematic diagram of guide RNA design targeting PCGF6 and genotypes of generated PCGF6-KO clones. The sgRNA-targeting sequences were highlighted in blue, and PAM sequences are in red. The below schematic diagram showing the genotype of the two PCGF6 knockout clones (178bp and 203bp deletion respectively). **b.** Genotyping analysis of PCGF6 knockout human PSCs by PCR (n = 3). **c.** Relative expression level of *PCGF6* in the wild-type (WT) and PCGF6-KO human PSCs. The level of gene expression in the WT human PSCs is set as 1 (n = 3). **d.** Colony size of WT and PCGF6-KO cells (n = 80). **e.** Protein level of OCT4 and NANOG in WT and PCGF6-KO human PSCs; TUBULIN was used as loading control (n = 3). **f.** Protein level of PRC1.6 components (EHMT2, L3MBTL2, HDAC1, E2F6, MGA, RYBP, MAX) in WT and PCGF6-KO human PSCs;  $\alpha$ -TUBULIN was used as loading control (n = 3). **g-h.** Heatmap illustrating the RNA expression in WT and PCGF6-KO human PSCs for selected genes of pluripotency (**g**) and components of PRC complexes (**h**) based on RNA-seq analysis. TPM, Transcripts Per Kilobase Million. Each point represents a biological replicate. Data are presented as the mean  $\pm$  SD. Statistical significance was determined using the unpaired, two-tailed t-test in **c**, **d**, **e** (\* $p$ <0.05, \*\* $p$ <0.01, \*\*\* $p$ <0.001). Exact  $P$  values and statistical parameters are provided as a Source Data file.



## Supplementary Figure 2. PCGF6 regulates endoderm differentiation of human PSCs.

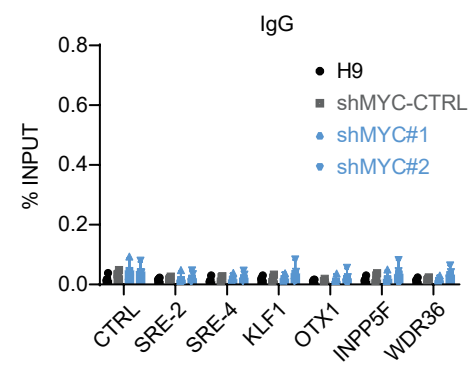
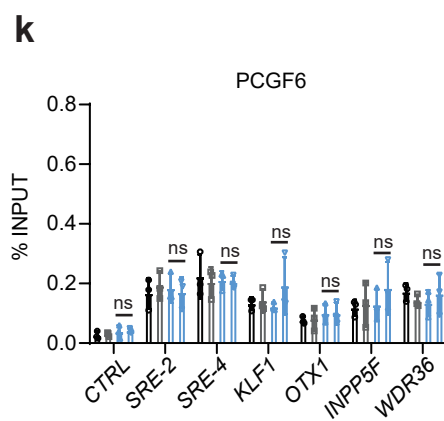
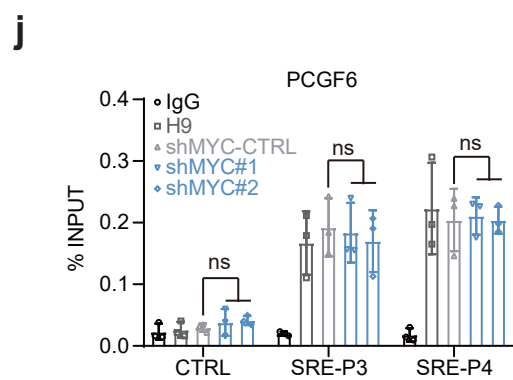
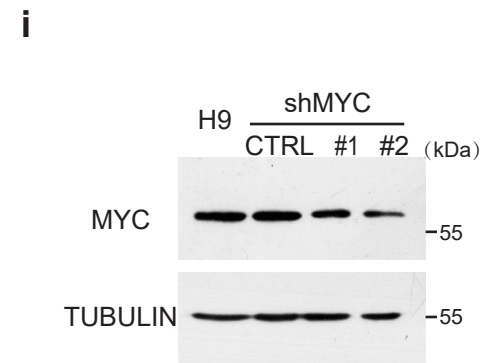
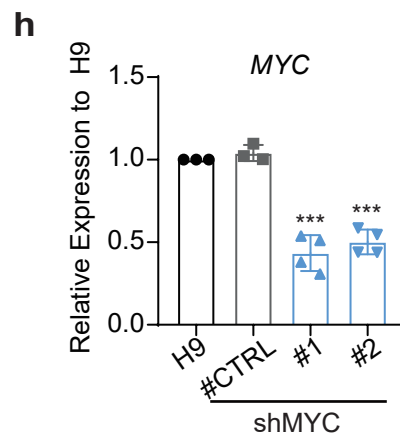
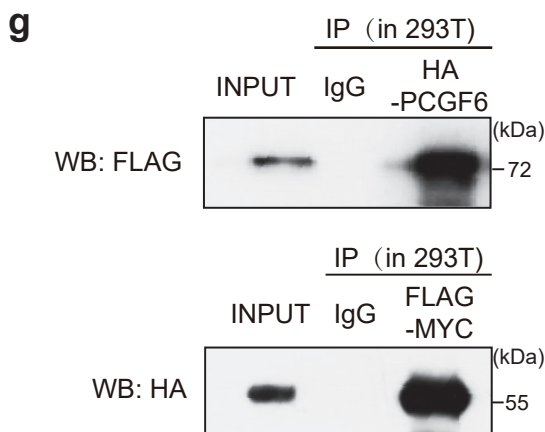
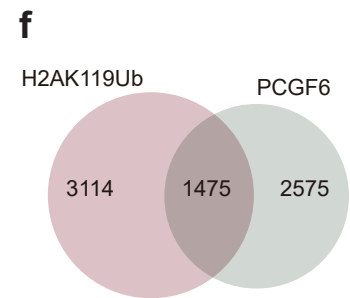
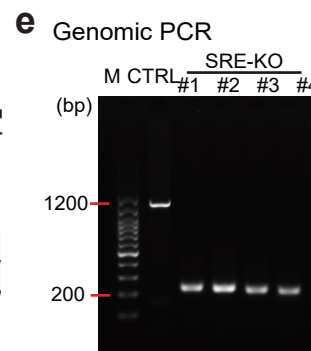
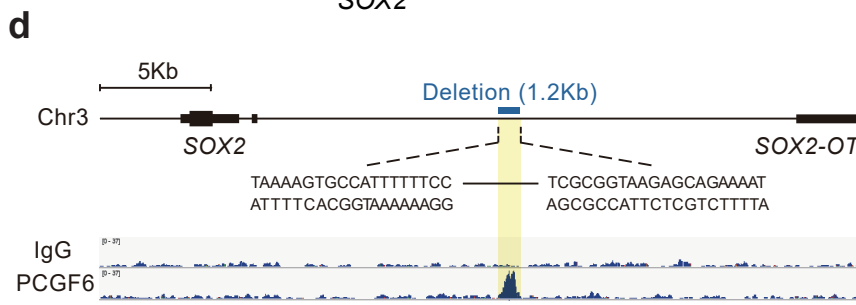
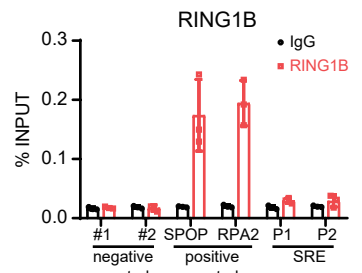
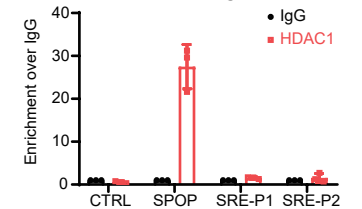
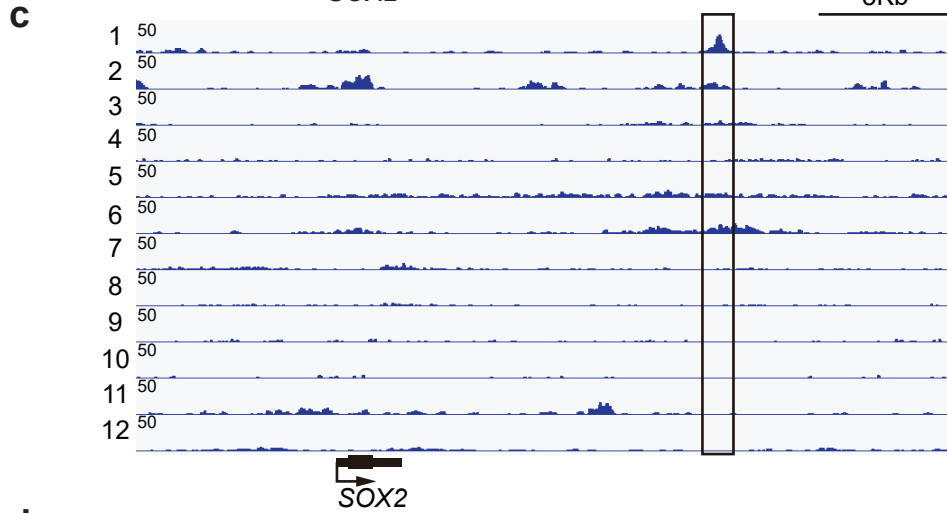
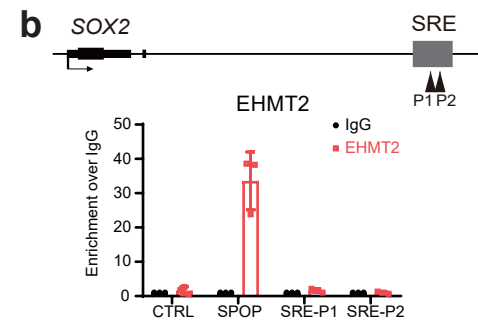
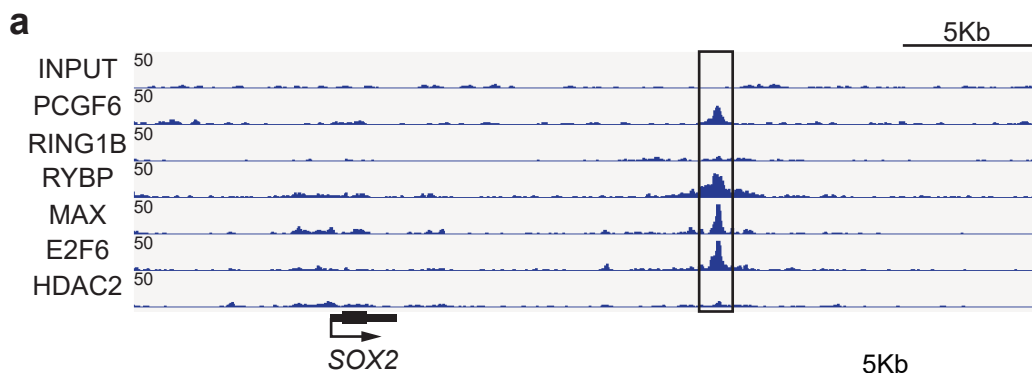
**a.** Schematic representation of definitive endoderm (DE) and pancreatic differentiation of human PSCs. **b.** qRT-PCR analysis for expression of endoderm markers (*FOXA2* and *SOX17*) in WT and PCGF6-KO human PSCs during endoderm differentiation. Results are shown relative to undifferentiated WT (n = 3). **c.** Left panel: Flow cytometric analysis showing the percentage of CXCR4-positive cells in differentiated WT and PCGF6-KO cells. Right panel: the percentage of CXCR4-positive cells was counted (n = 3). **d.** qRT-PCR analysis for expression of pancreatic markers (*PDX1*, *NKX6.1*, *HNF4A* and *CDX2*) in WT and PCGF6-KO human PSCs during pancreatic differentiation (n = 3). **e.** Immunostaining of the pancreatic marker (PDX1) in WT and PCGF6-KO cells after pancreatic differentiation (n = 3). Scale bars, 200  $\mu$ m. **f.** qRT-PCR analysis for expression of cardiac markers (*T*, *GATA4* and *NKX2.5*) in WT and PCGF6-KO human PSCs during cardiac differentiation (n = 3). **g.** Immunostaining of the cardiac marker (T) in WT and PCGF6-KO cells after cardiac differentiation (n = 3). Scale bars, 200  $\mu$ m. **h.** KEGG pathway analysis of up-regulated genes in PCGF6-KO PSCs. The y axis shows the KEGG signaling pathway categories, the x axis refers to pathway enrichment. **i.** Venn diagram showing the overlap of PRC1.6 targets in WT cells and up-regulated PCGF6 targets in PCGF6-KO cells. **j.** The heatmap showing the enrichment of PCGF6, RYBP, RING1B, MAX (WT and PCGF6-KO), E2F6 (WT and PCGF6-KO) and H2AK119ub (WT and PCGF6-KO) at PCGF6-related PRC1.6 targets in human PSCs. ChIP-seq data of RYBP and RING1B were obtained from GEO database GSM2805870 and GSM2805868, respectively. **k.** ChIP-qPCR analysis for RING1B, EHMT2 and HDAC1 binding at WNT genes (*FZD4*, *FZD9*, *RSPO4* and *AXIN2*) in human PSCs. IgG served as negative control. ChIP enrichments are normalized to Input (n = 3). Each point represents a biological replicate. Data are presented as the mean  $\pm$  SD. Statistical significance was determined using the unpaired, two-tailed t-test in **b-d**, **f**, **k** (\* $p$ <0.05, \*\* $p$ <0.01, \*\*\* $p$ <0.001). Exact  $P$  values and statistical parameters are provided as a Source Data file.





**Supplementary Figure 3. PCGF6 knockout delays pluripotency exits during neuroectoderm differentiation.**

**a.** Schematic representation of neuronal differentiation of human PSCs. **b.** qRT-PCR analysis for expression of pluripotent markers (*OCT4* and *NANOG*) in WT, PCGF6-KO and SOX2-rescue cells during neuroectoderm differentiation. Results are shown relative to undifferentiated WT (n = 2). **c.** Immunostaining of pluripotent markers (*OCT4* and *NANOG*) in WT, PCGF6-KO and SOX2-rescue cells after neuroectoderm differentiation (n = 3). Scale bars, 200  $\mu$ m. **d.** qRT-PCR analysis of *PCGF6* expression in WT, PCGF6-KO, PCGF6<sup>-/-</sup>+PCGF6 (PCGF6-KO/PCGF6 re-expressing) human PSCs. Results are shown relative to WT (n = 3). **e.** Protein level of PCGF6 and SOX2 in WT, PCGF6-KO and PCGF6<sup>-/-</sup>+PCGF6 human PSCs was evaluated and quantified; GAPDH was used as a loading control (n = 3). **f.** qRT-PCR analysis for expression of neural markers (*SOX1* and *PAX6*) in WT, PCGF6-KO and PCGF6<sup>-/-</sup>+PCGF6 cells during neuroectoderm differentiation (n = 3). **g.** Immunostaining of the neural progenitor markers (*SOX1* and *PAX6*) in WT, PCGF6-KO and PCGF6<sup>-/-</sup>+PCGF6 cells after neuroectoderm differentiation (n = 3). Scale bars, 200  $\mu$ m. **h.** qRT-PCR analysis for expression of neural progenitor marker (*SOX1*) and neuron markers (*NEUN* and *TUJ1*) in WT and PCGF6-KO human PSCs after neuron differentiation (21-days) (n = 3). **i.** Immunostaining of neural markers (*TUJ1* and *SOX1*) in WT, and PCGF6-KO cells after neuron differentiation (n = 3). Scale bars, 200  $\mu$ m. Each point represents a biological replicate. Data are presented as the mean  $\pm$  SD. Statistical significance was determined using the unpaired, two-tailed t-test in **b, d, f, h** (\* $p$ <0.05, \*\* $p$ <0.01, \*\*\* $p$ <0.001). Exact  $P$  values and statistical parameters are provided as a Source Data file.

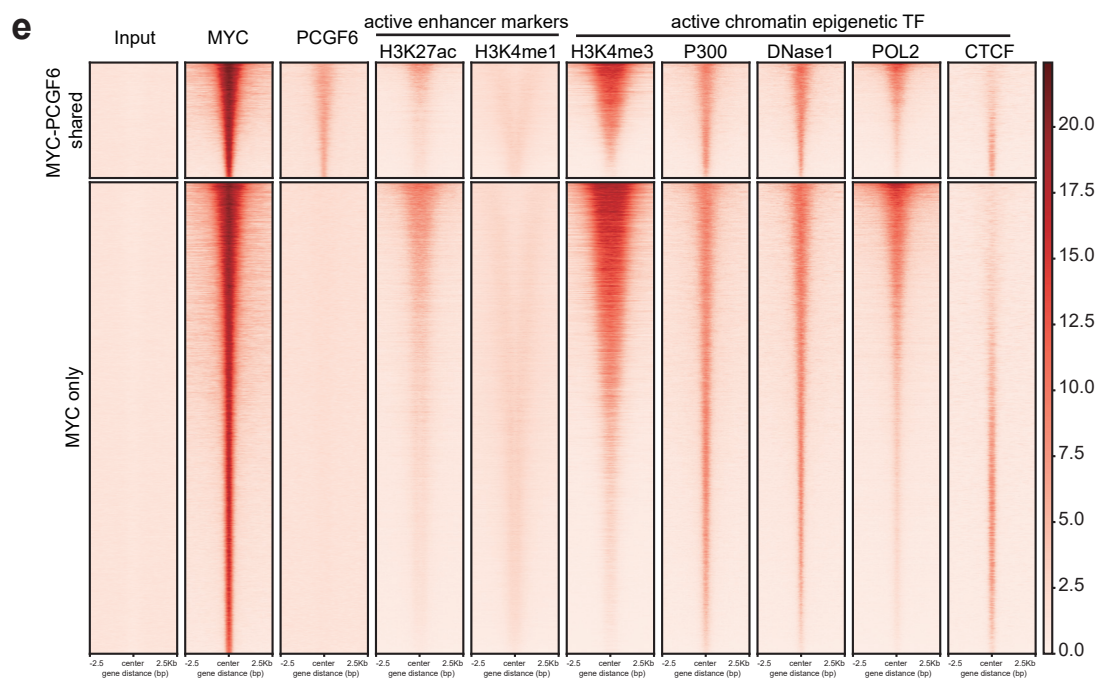
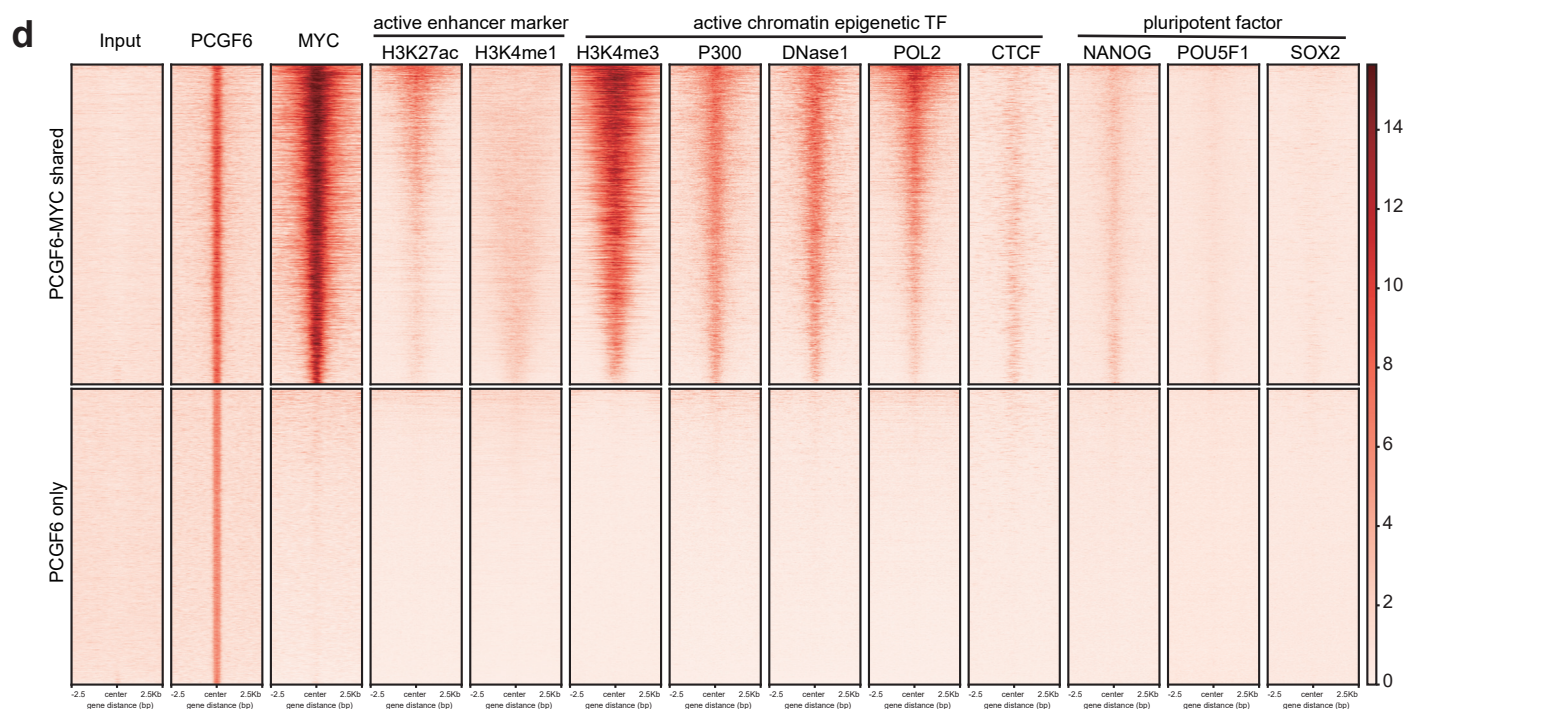
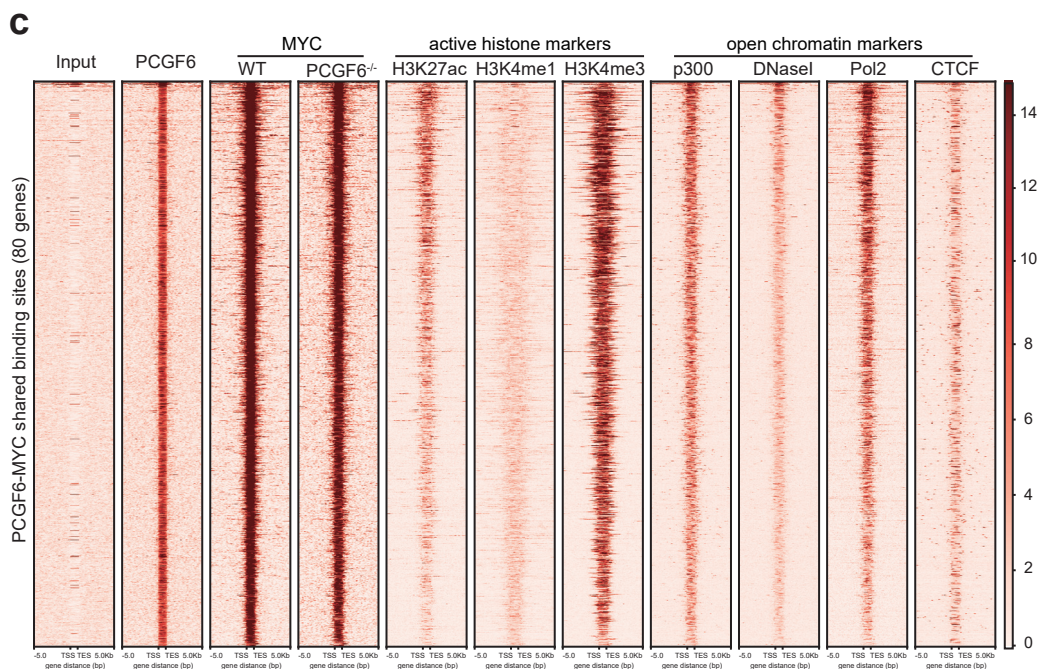
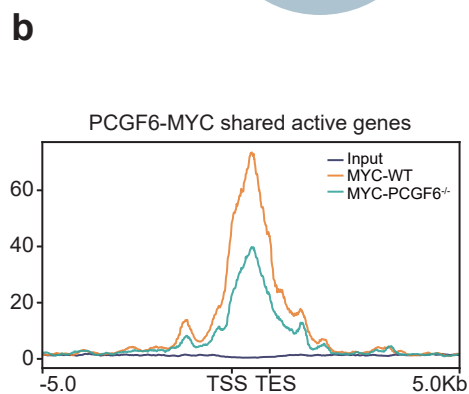
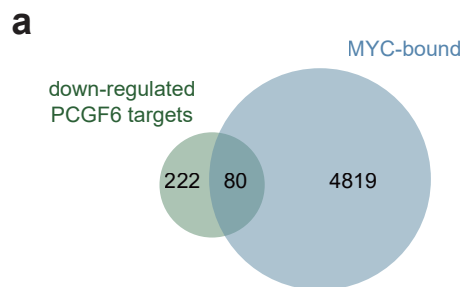


**Supplementary Figure 4. SRE-deficiency blocks neuroectoderm differentiation of human PSCs.**

**a.** Bedgraph for PCGF6, RING1B, RYBP, MAX, E2F6 and HDAC2 bound at *SOX2* locus. The x axis corresponds to genomic locations with the scale indicated at the top of panel, and the y axis corresponds to ChIP-seq signal intensity. **b.** ChIP-qPCR analysis for EHMT2, HDAC1 and RING1B binding at SRE locus in human PSCs. IgG served as negative control. (n = 3). Arrowheads represent the genomic position of qPCR primers. **c.** Bedgraph for RING1B bound at *SOX2* locus in different human cell lines. 1: PCGF6 ChIP-seq in this study; 2: H2AK119Ub ChIP-seq in this study; 3~12: RING1B ChIP-seq in human cell lines, including 3: H1 cell line (GSM2805868); 4: HUES64 cell line (GSM2805868); 5: WA09/H9 reprogramed naïve human PSCs (GSE164786); 6: WA09/H9 primed human PSCs (GSE164786); 7: Bone-marrow-derived primary human mesenchymal stem cells (hMSC) (GSE125166); 8: osteogenic cells derived from bone-marrow-derived primary human mesenchymal stem cells (hBMSC) (GSE125166); 9: ME-1 cell line (GSE128771); 10: HEK 293FT cells (GSE175673); 11: the human SCLC cell line (NCI-H1963, GSE191106); 12: human chronic myeloid leukemia cell line (K562, GSE167869). The x axis corresponds to genomic locations with the scale indicated at the top of panel, and the y axis corresponds to ChIP-seq signal intensity. **d.** Schematic diagram of guide RNA design targeting SRE. The sgRNA-targeting sequences were highlighted, and the deletion is depicted by horizontal blue box. **e.** Genotyping analysis of SRE knockout human PSCs (n = 3). **f.** Venn diagrams showing the overlap of PCGF6-activated genes and MYC-binding genes. The down-regulated PCGF6 targets means the overlap of down-regulated genes identified by RNA-seq and PCGF6 target genes identified by ChIP-seq. **g.** Co-immunoprecipitation assay in 293T cells with tagged PCGF6/MYC transfection (n = 3). **h.** qRT-PCR analysis for expression of *MYC* in the WT and MYC-knockdown human PSCs. Results are shown relative to wild-type H9 (n = 3). **i.** Western blot analysis of MYC in control and MYC-knockdown human PSCs.  $\alpha$ -TUBULIN served as a loading control (n = 3). **j-k.** ChIP-qPCR analysis of PCGF6-binding in WT and MYC-knockdown human PSCs at SRE (**j**) and other



PCGF6- and MYC-co-occupied target genes (*KLF1*, *OTX1*, *FOXO3*, *INPP5F* and *WDR36*) (**k**). ChIP enrichments are normalized to 100% input (n = 3). Each point represents a biological replicate. Data are presented as the mean  $\pm$  SD. Statistical significance was determined using the unpaired, two-tailed t-test in **b**, **h**, **j-k** (\* $p < 0.05$ , \*\* $p < 0.01$ , \*\*\* $p < 0.001$ ). Exact *P* values and statistical parameters are provided as a Source Data file.



**Supplementary Figure 5. Analyses of the co-occupancy of PCGF6 and MYC.**

**a.** The overlap of H2AK119ub binding genes and PCGF6 targets in human PSCs was displayed by Venn diagrams. The numbers showed the genes bound or co-bound by each protein identified by ChIP-seq. **b.** Tag density heatmaps illustrating changes of MYC bound in wildtype and PCGF6-KO human PSCs at PCGF6-MYC shared activated genes. **c.** Heatmaps for enrichment of PCGF6, MYC (WT and PCGF6-KO human PSCs), certain histone modifications (H3K27ac, H3K4me1 and H3K4me3) and transcription factors (P300, DNase1, Pol2 and CTCF) on PCGF6-MYC shared activated sites ( $\pm 2.5$  kb from the centers). ChIP-seq data were obtained from ENCODE human ESC ChIP-seq. **d.** Heatmaps for enrichment of PCGF6, MYC, certain histone modifications (H3K27ac, H3K4me1 and H3K4me3), transcription factors (P300, DNase1, Pol2 and CTCF) and pluripotent factors (NANOG, POU5F1 and SOX2) on PCGF6-MYC shared sites or PCGF6 only sites ( $\pm 2.5$  kb from the centers). ChIP-seq data were obtained from ENCODE human ESC ChIP-seq. **e.** Heatmaps for enrichment of PCGF6, MYC, certain histone modifications (H3K27ac, H3K4me1 and H3K4me3), transcription factors (P300, DNase1, Pol2 and CTCF) on PCGF6-MYC shared sites or MYC only sites ( $\pm 2.5$  kb from the centers). ChIP-seq data were obtained from ENCODE human ESC ChIP-seq.

**Supplementary Table 1. Primers for qRT-PCR analyses**

| <b>Primer Name</b> | <b>Forward Primer 5' - 3'</b> | <b>Reverse Primer 5' - 3'</b> |
|--------------------|-------------------------------|-------------------------------|
| GAPDH              | AATGAAGGGGTCATTGATGG          | AAGGTGAAGGTCGGAGTCAA          |
| NANOG              | CCCCAGCCTTTACTCTTCCTA         | CCAGGTTGAATTGTTCCAGGTC        |
| PCGF6              | GGCCCGATCCTAGTGCG             | AATAAGCGGGTAAAGACCCAGG        |
| OCT4               | CAAAGCAGAAACCCTCGTGC          | TCTCACTCGGTTCTCGATACTG        |
| SOX2               | GTCATTTGCTGTGGGTGATG          | AGAAAAACGAGGGAAATGGG          |
| SOX17              | GCATGACTCCGGTGTGAATCT         | TCACACGTCAGGATAGTTGCAGT       |
| FOXA2              | GGAGCAGCTACTATGCAGAGC         | CGTGTTTCATGCCGTTTCATCC        |
| EOMES              | CACATTGTAGTGGGCAGTGG          | CGCCACCAAACCTGAGATGAT         |
| T                  | TATGAGCCTCGAATCCACATAGT       | TATGAGCCTCGAATCCACATAGT       |
| AXIN2              | CTGGTGCAAAGACATAGCCA          | AGTGTGAGGTCCACGGAAAC          |
| FZD9               | CGGCACCAACACAGAGAAG           | CGTAGACATAGCAAACGATGAC        |
| SYT11              | AGAGGAGGATGTCATGCTAGG         | GATGTAGGGGTCAGATCCCTG         |
| NLGN3              | ACAGTGGTGCTAAACCCGTC          | ATTGCCATAACTGGCGAGGAT         |
| PAX6               | TCCGTTGGAACCTGATGGAGT         | GTTGGTATCCGGGGACTTC           |
| SOX1               | ATTATTTTGCCCGTTTTCCC          | TCAAGGAAACACAATCGCTG          |
| PDX1               | TTAGGATGTGGACGTAATTCCTGTT     | GGCCACTGTGCTTGTCTTCA          |
| NKX6.1             | AGACCCACTTTTTCCGGACA          | CCAACGAATAGGCCAAACGA          |
| HNF4A              | ACTACATCAACGACCGCCAGT         | ATCTGCTCGATCATCTGCCAG         |
| CDX2               | CTGGAGCTGGAGAAGGAGTTTC        | ATTTTAACTGCCTCTCAGAGAGC       |
| GATA4              | CAGGCGTTGCACAGATAGTG          | CCCGACACCCCAATCTC             |
| NKX2.5             | CTCCCAACATGACCCTGAGT          | CTCATTGCACGCTGCATAAT          |
| TUJ1               | TGGATTTCGGTCCTGGATGTG         | ACCTTGCTGATGAGCAACGT          |
| MYC#1              | GGCTCCTGGCAAAAGGTCA           | CTGCGTAGTTGTGCTGATGT          |
| MYC#2              | TCCCTCCACTCGGAAGGAC           | CTGGTGCATTTTCGGTTGTTG         |

**Supplementary Table 2. Primers for ChIP-qPCR analyses**

| <b>Primer Name</b> | <b>Forward Primer 5' - 3'</b> | <b>Reverse Primer 5' - 3'</b> |
|--------------------|-------------------------------|-------------------------------|
| unbound control-1  | CAGACCAGCACTTTCGGTGT          | TTGTCCCAAACAAACCACC           |
| unbound control-2  | AGCTCAGGCCTCAAGACCTT          | AAGAAGATGCGGCTGACTGT          |
| SRE-P1             | TCATCCTCTTCAGGCAGCATT         | ACCAATATGGTGACCGTCTGAG        |
| SRE-P2             | GGTGGAAGCGTTTGTCTGATG         | GGCGTTTCGAAGGCACAG            |
| SRE-P3             | TATTTAGCAAGCCGGGACGG          | GGAAGGGGTGTGGTTACCG           |
| SRE-P4             | GAAACGAAAAAGCTCGCGGT          | TAACCGGCTATCGGTGATGC          |
| SRE-P5             | TGACCCGACTGTGGGTACTT          | AAATCAGCTGAAACCCGCCT          |